PHYSICAL REVIEW B **84**, 161411(R) (2011)

Superhard sp^3 carbon allotropes with odd and even ring topologies

Daniele Selli,[1] Igor A. Baburin,[1,2] Roman Martoňák,[3] and Stefano Leoni[1,*]

[1]*Technische Universität Dresden, Institut für Physikalische Chemie, D-01062 Dresden, Germany*

[2]*Max-Planck-Institut für Chemische Physik fester Stoffe, D-01187 Dresden, Germany*

[3]*Department of Experimental Physics, Comenius University, Mlynská Dolina F2, SK-842 48 Bratislava, Slovakia*

(Received 14 September 2011; published 25 October 2011)

Four sp^3 carbon allotropes with six, eight, and 16 atoms per primitive cell have been derived using a combination of metadynamics simulations and topological scan. A chiral orthorhombic phase *o*C16 ($C222_1$) was found to be harder than monoclinic *M*-carbon and shows excellent stability in the high-pressure range. A second orthorhombic phase of *Cmmm* symmetry, by ∼0.028 eV/atom energetically lower than *W*-carbon, can be formed from graphite at ∼9 GPa. In general, the mechanical response under pressure was found to depend on the structure topology, which reflects the way rings are formed from an initial graphene layer stacking.

DOI: 10.1103/PhysRevB.84.161411 PACS number(s): 61.50.−f, 61.66.−f, 64.70.K−, 81.05.U−

Introduction. The quest for carbon materials with improved mechanical properties and a tailored optical gap is a topic of high priority. Engineering unique properties is tightly connected with the ability to predict crystal structures, which remains a crucial issue in both basic solid-state research and modern materials science.[1]

In the effort of anticipating superior materials for catalysis, hydrogen storage, and gas segregation, structure prediction stands out for its capacity to efficiently indicate viable technological target compounds. The challenge consists in identifying metastable modifications that can exhibit interesting physical and chemical properties.

Compression of graphite at high pressure and temperatures produces diamond.[2] Graphite cold compression on the contrary produces a hard and transparent product, different either from cubic or hexagonal diamond,[3–9] but not fully characterized so far. Many recent studies deal with the nature of this metastable product. Several energetically competing carbon phases were proposed (*W*- and *M*-carbon,[10] bct C_4) as plausible structure solutions, based on estimating transition pressures, goodness of fit of x-ray diffraction data, and band gaps.[11–13] The intrinsic problem of stacking faults in the pristine graphite, and Raman evidence of amorphization suggest a mixture of different phases in the compressed material. The two energetically most preferable candidates so far (*M*- and *W*-carbon) can be described (in terms of topology) as corrugated graphene sheets interconnected by an alternating sequence of odd rings (pentagons and heptagons) fused into a 5 + 7 pattern. This odd-ring topology formally results from connecting puckered graphene layers aligned in a particular way. On the other hand, further compressing *M*- or *W*-carbon can produce different diamond polytypes. Therefore, a larger variety of intermediate hard structures can in principle be expected.

In this Rapid Communication, we further unfold the structural diversity of sp^3 carbon phases. We base our approach on metadynamics simulations of structural transformations[14,15] and topological enumeration to efficiently scan the configuration space. We report on energetic, mechanical, and electronic properties of four unique tetrahedral carbon phases, and insist on a different underlying graphitic pattern connected with the formation of a particular topology. We show how distinct topologies with 5 + 7 (odd-odd), but also 5 + 8 (odd-even) and 4 + 6 + 8 (even-even-even) ring patterns can do for different mechanical responses.

Methods. Efficient theoretical approaches to hypothetical carbon modifications, based, e.g., on random techniques, genetic (evolutionary) algorithms, or accelerated molecular dynamics (MD)[16] result in important discoveries supporting experiments.[17,18] In some approaches the use of graph theoretical methods[19] represents a means of increasing the sampling efficiency of carbon configurations. It was indeed a graph-theoretical approach that allowed to derive all possible sp^3 carbon allotropes with four atoms per cell (including the recently rediscovered bct C_4).[19] Metadynamics, on the other hand, explores the energy landscape along collective reaction coordinates, which in the case of high-pressure polymorphs is represented by the simulation box itself. While metadynamics does not require prior knowledge of the energy landscape under investigation, its sampling efficiency improves on combining many independent runs started from different initial configurations. Additionally, the number of atoms per simulation box is critical for capturing a particular atomic configuration. Diamond and lonsdaleite are important metastable forms of carbon. They can appear in the same metadynamics run only if the number of atoms in the box is at least four and multiples thereof. Similarly, including a minimum of three atoms (or multiples thereof) is sufficient to find a dense carbon with quartz topology, recently suggested from evolutionary algorithms.[20]

To systematically include known and find new carbon forms, metadynamics runs were performed on simulation boxes comprising three, four, six, eight, 12, and 16 carbon atoms, respectively. A similar approach has been shown to work well in connection with plain MD to search for ice phases.[21,22] Quasirandom four-connected nets were used as starting configurations. We note here that the application of metadynamics in this case is slightly different from its typical use for simulation of crystal-crystal structural phase transitions, as recently reviewed in Refs. 23 and 24. While in both cases the simulation cell is used as an order parameter, here one instead starts from a disordered configuration in a small cell and searches for low-energy configurations representing crystalline structures with a given number of atoms in the

unit cell. Each run typically consisted of ∼25 000 metasteps. Within each metastep MD was performed in the *NVT* ensemble for at least 0.5 ps at 300 K. In these preliminary scans the tight-binding Tersoff potential[25] was used, which ensured rapid and reliable structure evolution thanks to its good description of sp^2/sp^3 carbons. Molecular dynamics in the *NVT* ensemble was performed with the CP2K code.[26,27] Structure diversity was judged by calculating vertex symbols, which contain information on all the shortest rings meeting at each atom, and coordination sequences, as implemented in the TOPOS package.[28] Both topological descriptors are widely used, e.g., for the topological characterization of zeolites.[28] Metadynamics trajectories contained many foamlike structures with mixed sp^2-sp^3 carbon atoms and a few sp^3 allotropes. In the case of unique tetrahedral structure types, inferred from their topology, ideal space groups and asymmetric units were identified with the Gavrog Systre package.[29] In a subsequent set of runs, candidate structures were studied with respect to their transformability into diamond by metadynamics simulations using SIESTA[30,31] as the density functional theory (DFT)/MD layer.

In the initial metadynamics runs the choice of large pressure values is less critical. It is rather the number of atoms in the simulation box that decides whether a particular topology can be visited at all within a single metadynamics run. The structures presented in the following were harvested from metadynamics runs performed at 0 and 5 GPa, with six, eight, and 16 atoms in the simulations box.

On idealized structures variable-cell conjugate-gradient relaxation was performed within density functional theory [generalized gradient approximation (GGA), Perdew-Burke-Ernzerhof (PBE)] as implemented in the SIESTA package.[30,31] Electronic states were expanded by a double-zeta basis set with polarization functions (DZP). Core states ($1s^2$) were described by norm-conserving Troullier-Martins pseudopotentials.[32] The charge density was represented on a real-space grid with an energy cutoff of 200 Ry. Forces were relaxed to less than 0.01 eV/Å. Convergence with respect to the number of k points was carefully checked.

Results and discussion. Small boxes of two and three atoms expectedly produced cubic diamond and quartz, respectively. With four atoms both cubic and hexagonal diamond (lonsdaleite) were collected. From six, eight, and 16 atoms metadynamics three unique structures were found, two monoclinic (*m*C12 and *m*C32, Fig. 1) and one orthorhombic (*o*C16-I, Fig. 1). From further propagating *o*C16-I in metadynamics runs at 100 GPa, *o*C16-II (*Cmmm*) was found. Their symmetries and structural parameters are summarized in Table I. All phases correspond to a stacking of corrugated graphene layers interconnected by an alternating sequence of pentagons and heptagons (*o*C16-I and *m*C32, Fig. 1), as for *M*- and *W*-carbon. Alternatively, pentagons and octagons, or squares and octagons can also be placed between puckered graphitic layers as it is realized in *m*C12 and *o*C16-II, respectively (Fig. 1). Physical properties of the unique allotropes are compared with those of known structures in Table II. In terms of volume per atom, *o*C16-I is the densest, hardest structure, closely followed by *o*C16-II and *m*C12. With a calculated band gap of 4.5 eV, *o*C16-I is also the structure closest to diamond.

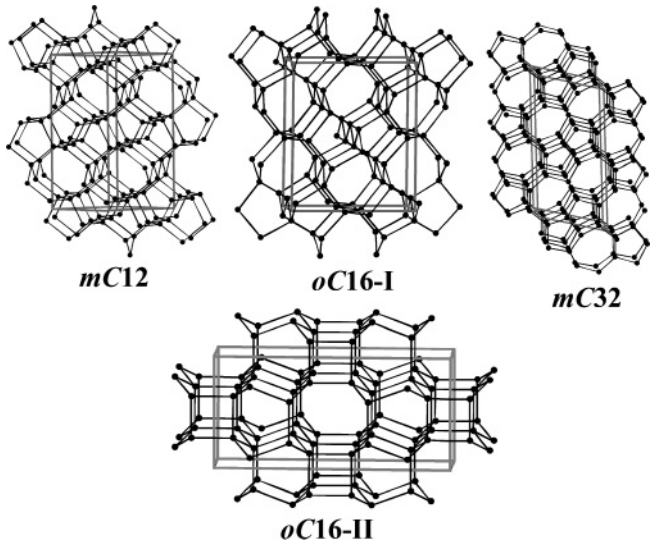

FIG. 1. Crystal structures of unique carbon phases. *o*C16-I and *m*C32 are characterized by a 5 + 7 odd-odd ring pattern. *m*C12 represents a distinct 5 + 8 odd-even ring topology, while *o*C16-II contains even rings only, 4 + 6 + 8.

The stability of different carbon phases in a wide pressure range is presented in Fig. 2. At elevated pressures, the found

TABLE I. Crystal structure information for unique carbon phases at 0 GPa.

Pearson symbol	Space group cell	Wyckoff position	x	y	z
*m*C12	$C2/c$				
	$a = 3.4242$; $b = 8.5218$;	4*e*	0	0.80280	3/4
	$c = 3.7012$; $\beta = 138.96°$	8*f*	0.84662	0.91988	0.95940
*m*C32	$C2/m$	8*j*	0.46444	0.68220	0.12680
	$a = 9.7242$; $b = 4.2932$;	8*j*	0.94998	0.68122	0.59997
	$c = 4.8617$; $\beta = 103.96°$	8*j*	0.30907	0.68472	0.43555
		8*j*	0.18908	0.68609	0.87688
*o*C16-I	$C222_1$	4*a*	0.43209	1/2	0
	$a = 6.6698$; $b = 5.5609$; $c = 2.5119$	4*b*	1/2	0.08196	1/4
		8*c*	0.81701	0.76297	0.11960
*o*C16-II	*Cmmm*	8*p*	0.66672	0.68505	0.0
	$a = 8.8134$; $b = 4.2743$; $c = 2.5281$	8*q*	0.58903	0.81586	1/2

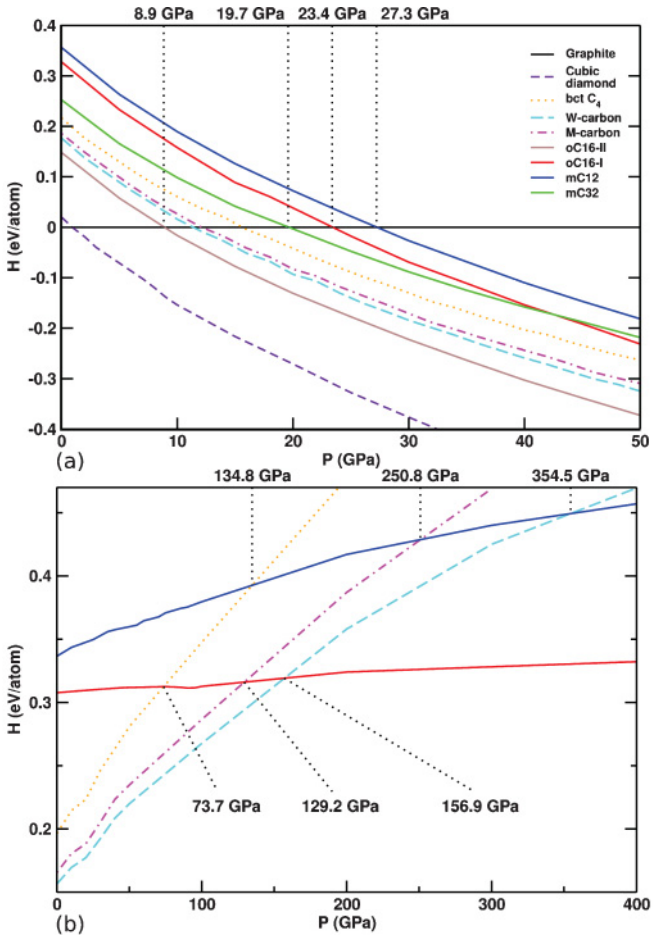

FIG. 2. (Color online) (a) Enthalpies (relative to graphite) of different carbon allotropes; (b) enthalpies of certain sp^3 carbon allotropes (relative to diamond) in the high-pressure range. The colors (lines) are the same as in (a).

allotropes become more stable than graphite [Fig. 2(b)]. The transition pressures are similar for the *m*C32 and *o*C16-I structures (19.7 and 23.4 GPa, respectively) and much higher (by 10 GPa) for *m*C12. *m*C12 and particularly *o*C16-I are stabilized upon increasing pressure. Furthermore, the stability of *o*C16-I remains basically constant (up to 400 GPa) whereas *M*- and *W*-carbon rapidly become energetically unfavorable above 100 GPa.

Bulk moduli (B_0) were obtained by fitting the total energy as a function of volume to the third-order Birch-Murnaghan equation of state (Table II). Strikingly, *o*C16-I is harder than *M*- and *W*-carbon, although it is less stable below 129.2 GPa (Fig. 2). On the contrary, *o*C16-II features a lower enthalpy, but its gap is nonetheless intermediate between lonsdaleite and bct C_4, which is structurally also the case. By inspection of Fig. 1, the motifs of lonsdaleite and bct C_4 can be easily recognized.

TABLE II. Calculated equilibrium volumes (V_0), bulk moduli (B_0), band gaps (E_g) and hardness (H).

Structure	Method	V_0 (Å^3)	B_0 (GPa)	E_g(eV)	H (GPa)[a]
Diamond	This work	5.79	424.2	4.19	87.3
	PBE (Ref. 20)	5.70	431.1	4.2	
*m*C12	This work	5.91	399.5	2.82	84.4
*o*C16-I	This work	5.82	411.0	4.5	85.8
*m*C32	This work	6.16	384.5	3.47	70.2
*o*C16-II	This work	5.95	408.4	3.15	84.4
W-carbon	This work	6.04	391.8	4.35	83.1
M-carbon	This work	6.06	392.6	3.51	82.7
	PBE (Ref. 20)	5.97	392.7	3.60	
bct C_4	This work	6.11	393.4	2.6	82.0
	PBE (Ref. 20)	6.01	411.4	2.7	

[a]According to the method of Lyakhov and Oganov (Ref. 33).

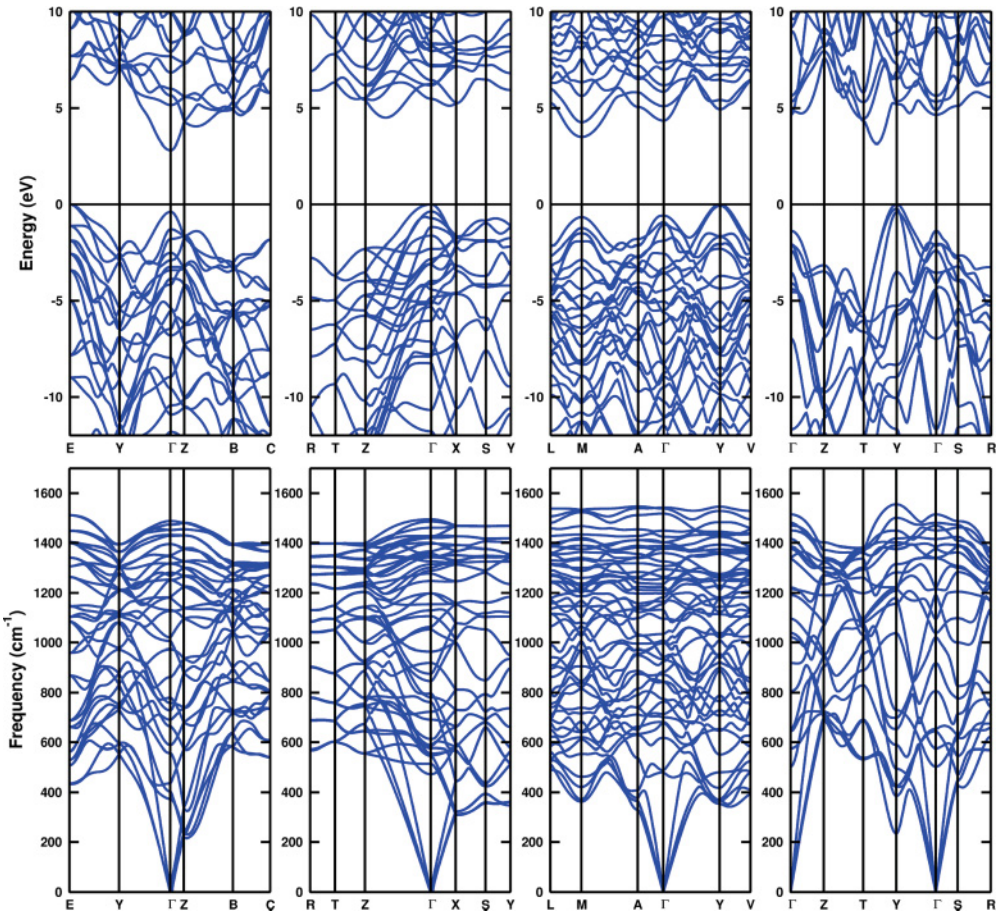

FIG. 3. (Color online) Electronic band structures (top) and phonon dispersion curves (bottom) for (from left to right) *m*C12, *o*C16-I, *m*C32, and *o*C16-II carbon phases.

The electronic band structures of *m*C12, *o*C16 (I and II), and *m*C32 at 50 GPa are shown in Fig. 3. The structures are insulating with indirect band gaps in the range 2.8–4.5 eV. The gaps do not depend on the pressure up to 50 GPa. All the gaps are smaller than in diamond, but similar to those of *M*- and bct-carbon.

Phonon dispersion curves were calculated within a pressure range up to 100 GPa. No imaginary frequencies were observed throughout the whole Brillouin zone, confirming the dynamical stability of the intermediate sp^3 structures (Fig. 3). Isothermic-isobaric molecular dynamics simulations (300 K, 1 atm, 3 ps) also confirmed the stability of the found phases.

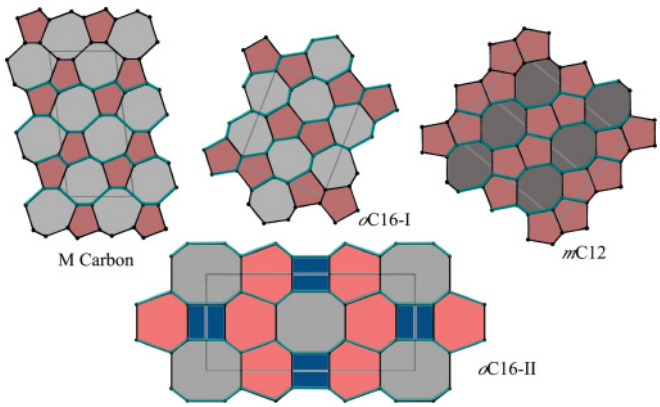

FIG. 4. (Color online) Comparison of *M*-carbon with *o*C16-I, *m*C12, and *o*C16-II with respect to their underlying puckered graphitic stacking. Layers are highlighted in turquoise (medium gray).

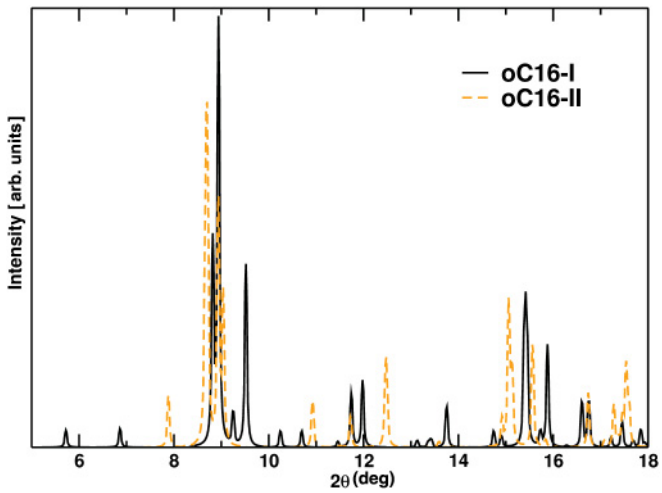

FIG. 5. (Color online) Simulated XRD pattern for *o*C16-I and *o*C16-II carbon phases ($\lambda = 0.3329$ Å). The structural data are those of Table I.

Figure 4 shows the relation between the discovered structures and the graphene layer stackings they are derived from. This information can be obtained by deconstructing the structures and looking for graphitic layers within the lattices. For the unique structures, the matching we are presenting is supported by the metadynamics runs, where a (fully or partially) graphitic structure is a typical precursor of the sp^3 phases, along the simulation time coordinate.

In general, we notice that hardness and band gap are diversely distributed among the phases. In the effort of providing an answer to the outstanding question of hard and transparent sp^3 carbon, *o*C16-II and *o*C16-I appear as better candidates as hitherto suggested, the former particularly for its stability, for a really transparent band gap and hardness the latter. In Fig. 5 we present the simulated x-ray diffraction (XRD) patterns of *o*C16-I and *o*C16-II. With reference to the experimental pattern,[8] the relevant regions between 8.5° and 10° as well as 14.5° and 17° are similarly populated. Intermediate peaks between 10° and 14° can better distinguish between the two structures, but are, however, depleted in the experiments[8] such that the experimental match is substantially the same for *o*C16-I and *o*C16-II.

Since superhard graphite is not synthesized from the gas phase, which would probably produce *o*C16-II as the only product due to its lowest enthalpy, in the real experiment much will depend on the nature of the starting graphitic material, and on the particular nucleation history, which would favor one pattern at the stage of phase growth. In this context, the overall stability of a particular structure is not the only parameter. The importance of this point of view has been recently pointed out,[34] and dedicated investigations are ongoing.

In conclusion, we have presented four sp^3 carbon materials, derived from combining metadynamics and topology to achieve higher scan efficiency. Two structures, *o*C16-I and *o*C16-II, stand out for hardness and band gaps, and should be considered in assessing the nature of the product of graphite cold compression.

Acknowledgments. R.M. was supported by the Slovak Research and Development Agency under Contract No. APVV-0558-10 and by the project implementation 26240120012 within the Research & Development Operational Programme funded by the ERDF. S.L. thanks the DFG for support under the priority project SPP 1415, as well as ZIH Dresden for the allocation of computational resources. Finally, we thank A. R. Oganov for inspiring discussions.

*stefano.leoni@chemie.tu-dresden.de

[1] R. Martoňák, A. R. Oganov, and C. W. Glass, Phase Transitions **80**, 277 (2007).
[2] T. Irifune, A. Kurio, S. Sakamoto, T. Inoue, and H. Sumiya, Nature (London) **421**, 599 (2003).
[3] W. Utsumi and T. Yagi, Science **252**, 1542 (1991).
[4] M. Hanfland, K. Syassen, and R. Sonnenschein, Phys. Rev. B **40**, 1951 (1989).
[5] T. Yagi, W. Utsumi, M. A. Yamakata, T. Kikegawa, and O. Shimomura, Phys. Rev. B **46**, 6031 (1992).
[6] M. Hanfland, H. Beister, and K. Syassen, Phys. Rev. B **39**, 12598 (1989).
[7] Y. X. Zhao and I. L. Spain, Phys. Rev. B **40**, 993 (1989).
[8] W. Mao, H. K. Mao, P. J. Eng, T. P. Trainor, M. Newville, C. C. Kao, D. L. Heinz, J. F. Shu, Y. Meng, and R. J. Hemley, Science **302**, 425 (2003).
[9] K. J. Takano, H. Harashima, and M. Wakatsuki, Jpn. J. Appl. Phys., Part 2 **30**, L860 (1991).
[10] A. R. Oganov and C. W. Glass, J. Chem. Phys. **124**, 244704 (2006).
[11] Q. Li, Y. Ma, A. R. Oganov, H. Wang, H. Wang, Y. Xu, T. Cui, H.-K. Mao, and G. Zou, Phys. Rev. Lett. **102**, 175506 (2009).
[12] J. T. Wang, C. Chen, and Y. Kawazoe, Phys. Rev. Lett. **106**, 075501 (2011).
[13] K. Umemoto, R. M. Wentzcovitch, S. Saito, and T. Miyake, Phys. Rev. Lett. **104**, 125504 (2010).
[14] R. Martoňák, A. Laio, and M. Parrinello, Phys. Rev. Lett. **90**, 075503 (2003).
[15] R. Martoňák, D. Donadio, A. R. Oganov, and M. Parrinello, Nat. Mater. **5**, 623 (2006).
[16] A. R. Oganov, *Modern Methods of Crystal Structure Prediction* (Wiley-VCH, Berlin, 2011).
[17] A. R. Oganov, J. Chen, C. Gatti, Y. Ma, Y. Ma, C. W. Glass, Z. Liu, T. Yu, O. O. Kurakevych, and V. L. Solozhenko, Nature (London) **457**, 863 (2009).
[18] Y. Ma, M. Eremets, A. R. Oganov, Y. Xie, I. Trojan, S. Medvedev, A. O. Lyakhov, M. Valle, and V. Prakapenka, Nature (London) **458**, 182 (2009).
[19] R. T. Strong, C. J. Pickard, V. Milman, G. Thimm, and B. Winkler, Phys. Rev. B **70**, 045101 (2004).
[20] Q. Zhu, A. R. Oganov, M. A. Salvadó, P. Pertierra, and A. O. Lyakhov, Phys. Rev. B **83**, 193410 (2011).
[21] V. Buch, R. Martoňák, and M. Parrinello, J. Chem. Phys. **123**, 051108 (2005).
[22] V. Buch, R. Martoňák, and M. Parrinello, The J. Chem. Phys. **124**, 204705 (2006).
[23] R. Martoňák, in *Modern Methods of Crystal Structure Prediction*, edited by A. R. Oganov (Wiley-VCH, Berlin, 2010).
[24] R. Martoňák, Eur. Phys. J. B **79**, 241 (2011).
[25] J. Tersoff, Phys. Rev. B **39**, 5566 (1989).
[26] G. Lippert, J. Hutter, and M. Parrinello, Mol. Phys. **92**, 477 (1997).
[27] G. Lippert, J. Hutter, and M. Parrinello, Theor. Chem. Acc. **103**, 124 (1999).
[28] V. Blatov, IUCr CompComm Newsletter **7**, 4 (2006).
[29] O. Delgado-Friedrichs [http://gavrog.sourceforge.net], 2006.
[30] P. Ordejon, E. Artacho, and J. M. Soler, Phys. Rev. B **53**, 10441 (1996).
[31] J. M. Soler, E. Artacho, J. D. Gale, A. Garca, J. Junquera, P. Ordejon, and D. Sanchez-Portal, J. Phys. Condens. Matter **14**, 2745 (2002).
[32] N. Troullier and J. L. Martins, Phys. Rev. B **43**, 1993 (1991).
[33] A. O. Lyakhov and A. R. Oganov, Phys. Rev. B **84**, 092103 (2011).
[34] R. Z. Khaliullin, H. Eshet, T. D. Kühne, J. Behler, and M. Parrinello, Nat. Mater. **10**, 693 (2011).